第 48 卷 第 23 期/2021 年 12 月/中国激光 研究论文

中国激光

# 狭缝式自由旋涡气动窗口光学质量测量方法研究

董玉磊*，韦承甫，刘现魁，柳琪，任晓明
中国船舶重工集团公司第七一八研究所，河北 邯郸 056027

**摘要** 为了测量稳定运行时超声速自由旋涡气动窗口(ADW)产生的像差，评价 ADW 的光学性能，提出了一种基于一维自准直 Shack-Hartmann 传感器，用拼接法进行波前复原测量气动窗口的方法。采用 671 nm 光源作为测试光源，高帧频 CCD 面阵相机采集经 Shack-Hartmann 波前传感器聚焦的子光斑阵列，采用拼接法进行波前复原。讨论分析了波前像差中沿 $y$ 方向的倾斜量、波前峰谷(PV)值和均方根(RMS)值与气动窗口工作状态的对应关系。实验结果表明，压力稳定时长曝光 PV 值为 0.1729λ，RMS 值为 0.0578λ。实验数据说明了 Shack-Hartmann 传感器拼接法对测量 ADW 光学性能的可行性，对 ADW 的进一步优化和实际应用具有重要的工程指导意义。

**关键词** 测量；激光器；自由旋涡气动窗口；Shack-Hartmann 波前传感器；拼接法；光学质量
**中图分类号** TN248.5 **文献标志码** A **doi**：10.3788/CJL202148.2304003

## 1 引 言

高能化学激光器通过将提取的化学反应能量转化为光能，输出的激光束具有准直性好和功率密度高等优点。传统的激光器输出窗口常采用晶体材料，而晶体窗口随着激光器输出功率的提高弊端也逐渐显现。对中红外波段激光来说，至今仍没有一种晶体窗口在激光穿过时可避免体吸收效应导致的受热畸变甚至炸裂[1-2]，因此运用空气动力学对光腔盒进行密封的超音速自由旋涡气动窗口(ADW)得到了广泛应用[3-6]。气动窗口工作时，超音速气流形成的气幕对激光器进行密封。与此同时，作为“窗口”，气体介质产生像差，影响输出光束的光束质量[7-9]，因此对气动窗口光学质量的研究成为进一步提高气动窗口性能的必要条件。

常用的气动窗口光学质量测量方法有干涉法、远场法、剪切干涉法和 Shack-Hartmann 传感器模式法[10-15]等。干涉法在气动测量中建立的参考波前对环境要求较高；远场法只能给出激光光束的宏观特性，无法量化波前像差，不利于气动窗口的优化设计；剪切干涉法得到的干涉条纹是波前差分的结果，条纹判读困难，波前复原运算量大；根据激光器需求，当前气动窗口设计的通光口径是尺寸为 280 mm×10 mm 的长矩形，采用 Zernike 多项式进行波前复原的 Shack-Hartmann 传感器模式法不再适用。本文待测量的气动窗口长宽比大，工作时产生较大环境噪音，为在此复杂环境中定量测量大长宽比气动窗口光学质量，定量分析波前像差，需要研究一种针对狭缝型气动窗口的光学质量检测方法，为气动窗口能否投入工程应用提供参考。

根据以往的气动窗口光学质量的测量和工程应用的经验[16-17]，对于其产生的像差成分有初步的了解。在此基础上，本文研究了一种用自准直 Shack-Hartmann 传感器测量波前，拼接法进行复原的 Hartmann 拼接法，并用 671 nm 光源进行实验验证。对比分析了气动窗口未工作时和压力稳定时的波前峰谷(PV)值和均方根(RMS)值，说明了 Hartmann 拼接法测量气动窗口光学质量方案的可行性。实验结果对气动窗口的进一步优化和工程应用具有重要指导意义，同时为分析大长宽比光斑光束质量提供了新的思路。

**收稿日期**：2021-02-23；**修回日期**：2021-03-17；**录用日期**：2021-04-30
**基金项目**：国家 863 计划(51326010201)
**通信作者**：*csscdyl@163.com

## 2　实验原理

### 2.1　实验装置

图 1 为自准直 Hartmann 拼接法测量气动窗口的光路示意图。自准直 Shack-Hartmann 传感器包括光源、分光棱镜、透镜组、缩束器、Shack-Hartmann 波前传感器、CCD 相机和标准平面镜。待测量气动窗口的通光口径为 280 mm×10 mm，压比为 100，工作气体为 $N_2$。671 nm 光源经透镜组、分光棱镜、缩束器后扩束为直径为 300 mm 的环形光斑，光平行于气动窗口的光学通道，并垂直于标准平面镜入射后原向返回，完成自准直过程。由于气动窗口将光斑尺寸限制为 280 mm×10 mm，原向返回的狭缝型光斑缩束后经微透镜阵列聚焦，在 CCD 上成像。

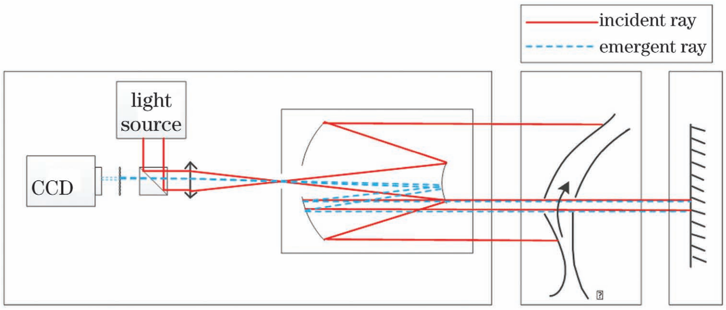


图 1　Hartmann 拼接法测量气动窗口光学质量光路示意图

Fig. 1　Optical path of Hartmann splicing method to measure ADW's optical quality

所采用的自准直 Shack-Hartmann 波前传感器的微透镜数目为 24×24 个，对应未缩束前直径为 300 mm 的光斑，每 10 mm 的光斑仅占 0.8 个子孔径，因此 280 mm×10 mm 长矩形光束经微透镜后聚焦为一列子光斑。为获得尽可能多的子光斑，避免缩束器次镜遮拦对采样点数的影响，将 Shack-Hartmann 传感器偏心使用，如图 2 所示。

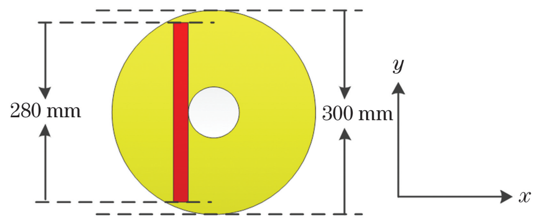


图 2　偏心用 Shack-Hartmann 波前传感器

Fig. 2　Decentred using of the Shack-Hartmann wavefront sensor

所用 CCD 采集帧频为 120 Hz，气动窗口工作时长为 2 s，有效子孔径有 22 个，成像结果如图 3(a)所示。波前无畸变时，经微透镜聚焦后的子光斑周期一致且稳定，气动窗口工作后由于介质超音速流动的影响，波前发生畸变，各子光斑随之出现偏移。拼接法根据实际光斑质心位置相对参考光斑的偏移量复原出各子波前，再根据波前的连续性，对子波前进行拼接，进而复原出完整波前。图 3(b)是在一个维度上进行子波前拼接的示意图。

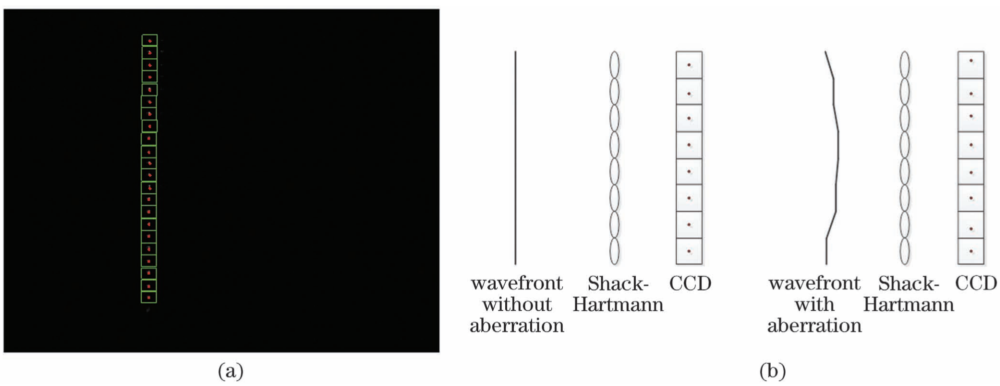


图 3　拼接法复原波前。(a)Shack-Hartmann 波前传感器光斑图；(b)波前有无畸变拼接复原图

Fig. 3　Splicing method to rebuild wavefront. (a) Facula of Shack-Hartmann wavefront sensor; (b) splicing method to rebuild wavefront with and without aberration

### 2.2　实验方法

在每个子孔径内，畸变波前的光斑质心相对于参考位置的偏移由斜率构成，斜率计算公式为

$$G_y=\left(\frac{\sum_{i=1}^{n}\sum_{j=1}^{n}I_{i,j}\times y_j}{\sum_{i=1}^{n}\sum_{j=1}^{n}I_{i,j}}-y_{\mathrm{ref}}\right)\times\delta\div F,\quad(1)$$

式中：$I$ 为灰度值；$(x_i, y_j)$ 为当前子孔径内像素点坐标；$n$ 为子孔径内像素维度；$(x_{\mathrm{ref}}, y_{\mathrm{ref}})$ 为参考位置坐标；$\delta$ 为 CCD 像素尺寸；$F$ 为透镜焦距。

子波前可以通过当前子孔径内的倾斜量复原出来，表达式为

$$\varphi = G_y \times y。\tag{2}$$

由于波前是连续的，完整波前则由各个子波前拼接而成。拼接子波前示意图如图 4 所示，其中 $x$ 和 $y$ 轴为矩形波前的长和宽，$z$ 轴为复原波前相对于标准平面波的变化量。同时，文献[17]说明了气动窗口产生的像差主要为倾斜、离焦和像散。倾斜像差可以通过一定的方式校正，而一列光斑无法计算其像散像差，因此本文计算的复原波前光学质量是减去整体倾斜后主要像差成分为离焦像差的 PV 值和 RMS 值。

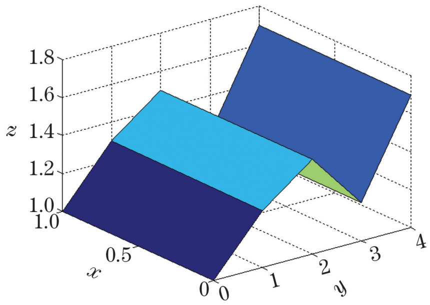


图 4 子波前拼接示意图

Fig. 4 Schematic of splicing sub-wavefront

## 3 分析与讨论

为方便观察复原波前在时间尺度和空间尺度上的变化，每个子孔径作为一个区域拼接复原波前，并将其按帧数顺序依次连接，结果如图 5 所示。

气动窗口工作前 1 s 触发 CCD 开始进行图像采集。$t_1$ 时刻气动窗口开始工作，$t_2$ 时刻压力达到设定值并开始保持稳定，$t_3$ 时刻工作结束。图 5 中的灰度值变化表示气动窗口复原波前在时间尺度和空间尺度上的 PV 值变化；时间尺度表征了波前随着气动窗口工作状态的变化而变化；空间尺度表征了气动窗口不同位置受气流扰动影响产生不同程度的畸变。为量化气动窗口波前像差，根据(1)式计算出采集全过程沿 $y$ 方向的整体倾斜量，并绘制整体倾斜量随气动窗口进气压力变化的曲线图，如图 6(a)所示。对复原波前减去整体倾斜处理前后的 PV 值如图 6(b)所示。

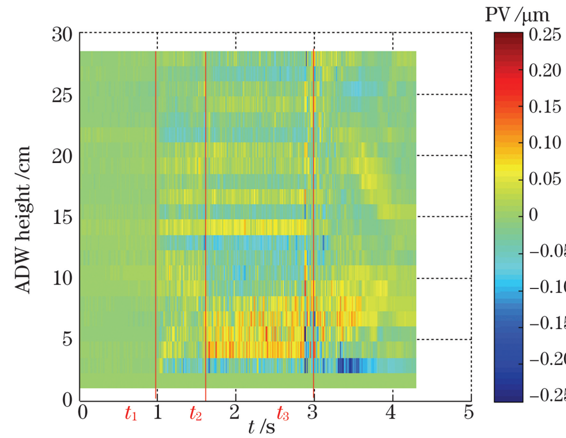


图 5 复原波前按帧数拼接的结果

Fig. 5 Splicing result of restored wavefront according to the number of frames

在 $0 \sim t_1$ 和 $t_2 \sim t_3$ 时进行长曝光处理，气动窗口未工作时沿 $y$ 方向的整体倾斜为 0.021 μrad，含整体倾斜的 PV 值为 0.0297λ，不含整体倾斜的 PV 值为 0.0212λ，RMS 值为 0.0074λ；气动窗口开始工作并压力达到稳定后，沿 $y$ 方向的整体倾斜为 0.3184 μrad，含整体倾斜的 PV 值为 0.2708λ，不含整体倾斜的 PV 值为 0.1729λ，RMS 值为 0.0578λ。气动窗口工作全过程下的复原波前光学质量如表 1 所示。

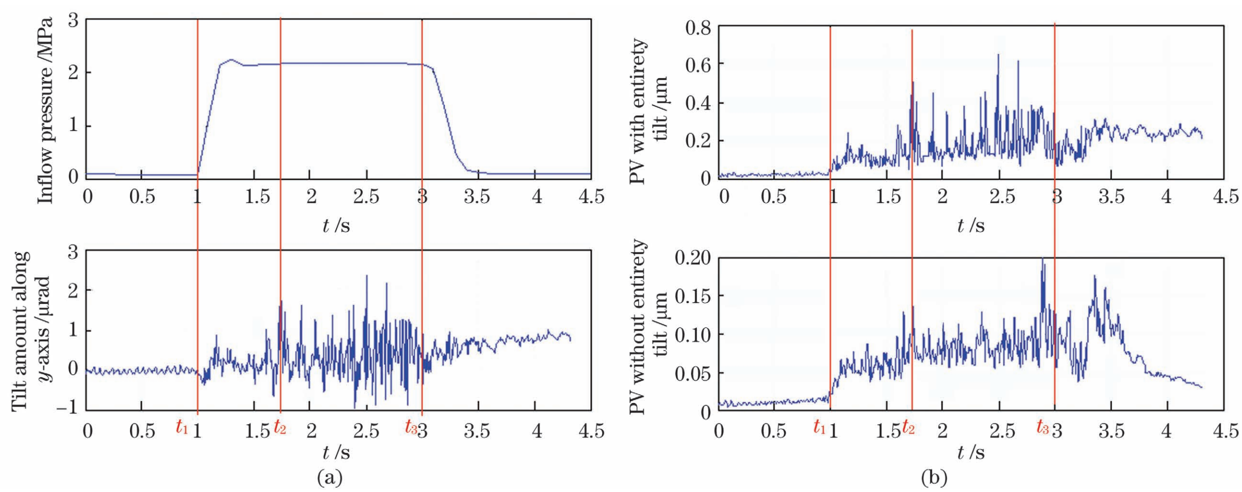


图 6 复原波前像差。(a)整体倾斜与进气压力；(b)减去整体倾斜前后的 PV 值

Fig. 6 Rebuilt wavefront aberration. (a) Entirety tilt and air inflow pressure; (b) PV value with and without entirety tilt

表 1 采集全过程气动窗口复原波前光学质量变化（λ=0.671 μm）

Table 1 ADW's rebuilt wavefront optical quality during total gather process(λ=0.671 μm)

| Condition | Tilt amount along $y$-axis/μrad | $PV_y/\lambda$ | $PV/\lambda$ | $RMS/\lambda$ |
|---|---|---|---|---|
| Before work | 0.021 | 0.0297 | 0.0212 | 0.0074 |
| Normal work | 0.3184 | 0.2708 | 0.1729 | 0.0578 |

图 7 为复原波前长曝光结果。长曝光图像的灰度值表示了气动窗口的当前状态。由于在气动窗口启动前 1 s 触发相机开始保存图像，因此未工作时长曝光时间为 1 s；根据整体倾斜像差可知，气动窗口稳定工作时长为 1.3 s，因此压力稳定时长曝光时间为 1.3 s。从图 7 可以看出，压力稳定时的复原波前长曝光说明气动窗口的 0～10 cm 区域内气流扰动带来的像差较大，是进一步优化的方向。但整体 PV 值仍控制在不到半个波长，说明气动窗口满足工程应用需求。

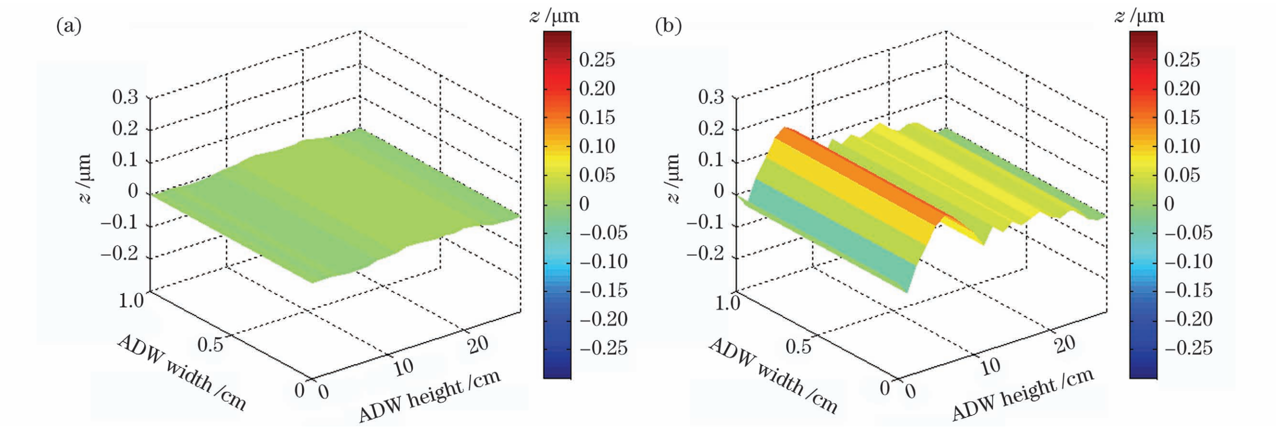


图 7 复原波前长曝光。(a)未工作时；(b)稳定工作时

Fig. 7 Rebuilt wavefront's long exposure. (a) Before work; (b) operating stably

## 4 结 论

根据以往气动窗口的测量结果和工程应用经验，气动窗口对光学质量的影响主要体现为倾斜、离焦和像散像差。采用 671 nm 光源，偏心用一维 Shack-Hartmann 波前传感器对气动窗口进行测量，在 CCD 上得到一列光斑。针对这一列光斑，提出了一种用拼接方式复原波前的方法，该方法能够计算倾斜像差，弥补了 Shack-Hartmann 传感器模式法不适用窄条形光斑的局限性。对比分析了气动窗口未工作时和压力正常时的复原波前长曝光像差，PV 值从 0.0212λ 变化至 0.1729λ，RMS 值从 0.0074λ 变化至 0.0578λ。这些数值有助于气动窗口的进一步优化，对气动窗口的实际应用具有重要的工程指导意义。同时，需要更高阶的自准直 Shack-Hartmann 传感器解决尺寸限制导致气流方向的采样点数不够的问题，开展复原二维波前的相关工作。

## 参 考 文 献

[1] Lu Q S, Liu Z J, Jiang Z P, et al. Thermal effect of laser windows on the beam divergent angle[J]. High Power Laser & Particle Beams, 1993, 5(2): 303-308.
陆启生，刘泽金，蒋志平，等. 激光窗口热效应对光束发散角的影响[J]. 强激光与粒子束，1993，5(2)：303-308.

[2] Chen J B, Liu Z J, Jiang Z P, et al. Heating effect of DF laser unstable cavity window and its affect on far-field optical spot[J]. High Power Laser & Particle Beams, 1994, 6(2): 243-249.
陈金宝，刘泽金，蒋志平，等. 非稳腔 DF 激光窗口热效应及其对远场光斑的影响[J]. 强激光与粒子束，1994，6(2)：243-249.

[3] Liu T H, Jiang Z F, Wei C H, et al. Design principle of the free-vortex aerodynamic window and an experimental study on its running properties[J]. Chinese Journal of Lasers, 2000, 27(1): 23-27.
刘天华，姜宗福，韦成华，等. 自由旋气动窗口设计原理及其工作性能的初步实验研究[J]. 中国激光，2000，27(1)：23-27.

[4] Liu S T, Guo J Z, Liu Q, et al. Design and experiment of high pressure-ratio free-vortex aerodynamic window[J]. High Power Laser and Particle Beams, 2008, 20(11): 1846-1850.

刘盛田，郭建增，柳琪，等．大密封压比超音速自由旋气动窗口设计与试验研究[J]．强激光与粒子束，2008，20(11)：1846-1850．

[5] Malkov V M，Trilis A V，Savin A V，et al．One-stage free-vortex aerodynamic window with pressure ratio 100 and atmospheric exhaust[J]．Proceedings of SPIE，2005，5777：170-174．

[6] Zhang D，Lu F Y，Li X Y．Numerical simulation of the overall flow and design of the free- vortex aerodynamic window [J]．Infrared and Laser Engineering，2005，34(6)：687-690．
张舵，卢芳云，李翔宇．自由旋涡气动窗口设计以及全流场数值模拟[J]．红外与激光工程，2005，34(6)：687-690．

[7] Liu T H，Jiang Z F，Li W Y，et al．Study on the effect of similar lens of free-vortex aerodynamic window[J]．Chinese Journal of Lasers，2002，29(1)：16-20．
刘天华，姜宗福，李文煜，等．自由旋气动窗口的类透镜效应研究[J]．中国激光，2002，29(1)：16-20．

[8] Yi S H，Hou Z X，Li L C．The preliminary analysis of optical performance of aerodynamic window[J]．Laser & Infrared，2002，32(3)：168-170．
易仕和，侯中喜，李立春．自由旋涡气动窗口的光学特性研究[J]．激光与红外，2002，32(3)：168-170．

[9] Liu S T，Liu Q，Chen L，et al．Improving optical performance of the free-vortex aerodynamic window by $N_2$/He mixture[J]．Chinese Journal of Lasers，2010，37(4)：965-969．
刘盛田，柳琪，陈良，等．利用 $N_2$/He 混合气提高自由旋涡气动窗口的光学性能[J]．中国激光，2010，37(4)：965-969．

[10] Liu T H，Jiang Z F，Chen F X，et al．Discussion on measurement of aerodynamic windows' beam quality [J]．Infrared and Laser Engineering，2002，31(3)：261-266．
刘天华，姜宗福，陈付幸，等．高能激光器气动窗口光束质量测量方法探讨[J]．红外与激光工程，2002，31(3)：261-266．

[11] Liu T H，Li W Y，Jiang Z F，et al．Study on the optical properties of free-vortex aerodynamic window using far-field method[J]．High Power Laser & Particle Beams，2001，13(1)：9-14．
刘天华，李文煜，姜宗福，等．用远场法研究自由旋气动窗口的光学特性[J]．强激光与粒子束，2001，13(1)：9-14．

[12] Chen F X，Liu T H，Jiang Z F，et al．Shearing interferometric investigation on degradation of light beam quality by the aerodynamic window's flow field [J]．High Power Laser & Particle Beams，2001，13(6)：670-674．
陈付幸，刘天华，姜宗福，等．用剪切干涉法测气动窗口流场对光束质量的影响[J]．强激光与粒子束，2001，13(6)：670-674．

[13] Liu T H，Jiang Z F，Xu X J，et al．Study on the optical quality of the free-vortex aerodynamic window using Hartmann-Shack sensing [J]．High Power Laser & Particle Beams，2002，14(4)：536-540．
刘天华，姜宗福，许晓军，等．用 Shack – Hartmann 传感器法研究自由旋涡气动窗口光束质量[J]．强激光与粒子束，2002，14(4)：536-540．

[14] Liu T H，Jiang Z F，Liu Z J，et al．Method of evaluating optical quality of aerodynamic windows for high energy lasers[J]．High Power Laser & Particle Beams，2002，14(2)：193-196．
刘天华，姜宗福，刘泽金，等．高能激光器气动窗口光束质量的评价方法探讨[J]．强激光与粒子束，2002，14(2)：193-196．

[15] Liu T H．Engineering design and related studies on the free vortex aerodynamic windows of high energy lasers[D]．Changsha：National University of Defense Technology，2002．
刘天华．高能激光器自由旋涡气动窗口的工程设计及其相关研究[D]．长沙：国防科学技术大学，2002．

[16] Liu T H，Jiang Z F，Xu X J，et al．Preliminary study on the compensation of the wavefront deformation induced by free-vortex aerodynamic window using AO system[J]．High Power Laser & Particle Beams，2002，14(5)：664-668．
刘天华，姜宗福，许晓军，等．自由旋涡气动窗口自适应光学波前校正初步研究[J]．强激光与粒子束，2002，14(5)：664-668．

[17] Liu T H，Jiang Z F，Xu X J，et al．Study on the laser wavefront deformation induced by the free-vortex aerodynamic window for high energy lasers [J]．Chinese Journal of Lasers，2003，30(4)：289-294．
刘天华，姜宗福，许晓军，等．高能激光器自由旋涡气动窗口激光波前畸变的初步研究[J]．中国激光，2003，30(4)：289-294．

# Measuring Method of Slit Free-Vortex Aerodynamic Window Optical Quality

Dong Yulei*, Wei Chengfu, Liu Xiankui, Liu Qi, Ren Xiaoming

*The 718th Research Institute of China Shipbuilding Industry Co., Ltd., Handan, Hebei 056027, China*

## Abstract

**Objective** Chemical reaction energy is converted to optical energy using a high-energy chemical laser. Its laser beam has good collimation and a high-power density when it is exported. The classic laser's exporting window is normally made of crystalline material, but the crystalline window's corrupt practice gradually emerges as laser power increases. There is no one type of crystalline window for the middle-infrared band laser that can withstand temperature distortion without exploding due to bulk absorption. Consequently, the free-vortex aerodynamic window (ADW), which seals the optical antrum using aerodynamics, has been commonly used. When the ADW works, ultrasonic airflow can produce an air curtain to seal the optical antrum. Simultaneously, the quality of the output beam would be affected by the gaseous aberration medium formed as the "window." Thus, conducting a study concerning ADW's optical quality is necessary for further improving ADW's performance.

Interferometry, far-field method, shear interferometry, and the Shack-Hartmann (S-H) model method, among others, are available. The reference wavefront interferometry established during ADW's gauging requires an ideal environment; the far filed process only provides the macroscopic property and cannot quantify the wavefront aberration, putting ADW's optimization design at a disadvantage; the obtained interferometric fringe shear interference is the result of wavefront difference, in which interpreting both fringes and wavefronts is difficult. The clear aperture of the currently proposed ADW is 280 mm × 10 mm, which is a large rectangle. Therefore, the S-H model approach, which uses the Zernike polynomial to rebuild the wavefront, is not appropriate. The unscanned ADW has a large length-width ratio in the paper, resulting in considerable environmental noise. An ADW optical quality detection method that can provide a reference for ADW's engineering application is required for measuring big length-width ratio ADW's optical quality in such a complex environment, quantitative analysis wavefront aberration; it should also provide a reference for ADW's engineering application and have the potential to aid in the future optimization of ADW.

**Methods** According to the past ADW optical quality measurement and engineering application experience, the preliminary knowledge of ADW's aberration component is already available. On this basis, an S-H splicing method is investigated in this study, which uses autocollimation S-H to measure wavefront and splicing method to rebuild wavefront; 671-nm optical source is used to verify furthermore. The experiment discusses and analyzes the peak-to-valley (PV) and root-mean-square (RMS) values in restructured wavefront when ADW is not in use and ADW's working status is stable. This can explain the feasibility of S-H splicing method to measure ADW's optical quality and its great significance to ADW's optimization and engineering applications. The method also provides a new perspective to discuss big length-width ratio spot's optical quality. The autocollimation S-H includes a light source, beam splitter prism, a battery of lenses, beam zoom implements, S-H wavefront sensor, CCD camera, and standard plane mirror; the current designed ADW's clear aperture is 280 mm × 10 mm, the pressure ratio is 100, and the working gas is $N_2$. The 671-nm light source goes through a battery of lenses, beam splitter prism, and beam zoom to expand a 300-mm diameter annular facula. The facula's optical axis is parallel to ADW's optical thoroughfare, and the facula would return the way it came after the incident the standard plane mirror vertically, which is the autocollimation process. ADW imposes restrictions on facula's size to 280 mm × 10 mm; therefore, slit facula returns the way it goes through the microlens array to focus and then image on CCD after shrinking. The autocollimation S-H wavefront sensor was adopted in this study; its microlens' quantity is 24 × 24, corresponding to 300-mm diameter annular facula before shrinking, every 10 mm occupy 0.8 subaperture. Therefore, the 280 mm × 10 mm rectangle facula focuses on a subspot list after passing through the microlens. To obtain more subspot, avoid the beam zoom implements second mirror block's influence, the paper bias uses the S-H. The paper used a CCD camera's collecting frame frequency of 120 Hz, a 2-s working duration of ADW, and subaperture's quantity of 22. The subspot's period is coincident and stable after wavefront going through the microlens without aberration. After ADW work, wavefront suggests aberration because of the gas medium's supersonic flowing; each subspot appears offset with it. The splicing method rebuilds each subwavefront according to the offset between the actual spot center with reference spot center,

splices each subwavefront according to the wavefront's continuity, and rebuilds the whole wavefront.

**Results and Discussions** According to the measured result of the past ADW and engineering application experience, ADW's impact on optical quality is considerably reflected in tilt, defocus, and astigmatism aberration. This study uses a 671-nm light source; bias uses a one-dimensional autocollimation S-H wavefront sensor to measure ADW and form a list of spots on CCD (Fig. 1). The study aims at this list of spots and proposes the splicing method to rebuild the wavefront; simultaneously, it calculates the tilt aberration. This method covers the shortage that the S-H model method is unsuitable for silt facula (Fig. 3). The contrastive paper analyzes the rebuilt wavefront's long exposure aberration when ADW is not in use, and its pressure is normal, PV value changes from 0.0212λ to 0.1729λ, and RMS value changes from 0.0074λ to 0.0578λ (Fig. 6, Table 1). The experiment data contribute to ADW's further optimization and have great directive significance to ADW's engineering application.

**Conclusions** The paper deals with the rebuilt wavefront's long exposure when ADW is not in use and it has stable pressure. The former $y$ tilt amount is 0.021 μrad, the PV value with a tilt is 0.0297λ, the PV value without tilt is 0.0212λ, and RMS value without tilt is 0.0074λ. The latter $y$ tilt amount is 0.3184 μrad, the PV value with a tilt is 0.2708λ, and RMS value without tilt is 0.0578λ. The gray value of the long exposure image shows the ADW's current working status. The paper trigger CCD to save images 1 s ahead of ADW launch so that long exposure time is 1 s when ADW is not in use. According to tilt aberration, ADW's stably working time is 1.3 s, so that long exposure time is 1.3 s when ADW's pressure reaches the set value and remains stable. When ADW's pressure reaches the set value and remains stable, the rebuilt wavefront's long exposure explains that in ADW's 0–10 cm area, the aberration results are in a relatively large airflow. It is the direction of further optimization. While the whole PV value is controlled in less than half wavelength, it explains that the ADW meets engineering application requirements.

**Key words** measurement; laser; free-vortex aerodynamic window; Shack-Hartmann wavefront sensor; splicing method; optical quality

**OCIS codes** 120.0280; 120.4820